

## EVALUATION OF LITHOPHYSAL CONDUCTIVITY, DIFFUSIVITY, AND POROSITY MEASUREMENTS USING THE REKA METHOD

George Danko, Nipesh Shah, and Davood Bahrami

Mackay School of Mines

University of Nevada, Reno

Reno, NV 89557

(775) 784-4284

### ABSTRACT

A method is presented, based on the NUFT and REKA V1.1 software packages combination, to study the nature of non-steady-state heat flow during a single-borehole REKA thermal probe thermophysical measurement in solid as well as lithophysal rock formation. The results prove the principle of the REKA method application in lithophysal formation. The numerical evaluation results, based on the use of two qualified software packages, show that the presented REKA probe arrangement is correctly modeled and that the effective heat conductivity and the lithophysal porosity can be evaluated correctly using the REKA probe method.

### INTRODUCTION

Site Recommendation design for Yucca Mountain [1] locates approximately 70% of the active emplacement and heat dissipation area of the potential repository in lithophysal rock formations. It is necessary to evaluate the thermophysical properties (heat conductivity,  $k$ , and thermal diffusivity,  $\alpha$ ) as well as the lithophysal porosity ( $\phi_l$ ) to support temperature and humidity calculations for both pre-closure and post-closure performance verifications at Yucca Mountain (YM).

In situ thermal probe measurements involving a large rock volume and mass provide valuable information about the lithophysal formation where the lithophysae distribution and the complex geometry has a primary effect upon the flow of heat. The single-borehole, in situ Rapid Evaluation of K and Alpha (REKA) method, that has been used successfully at other locations at YM since 1995 [2,3,4], is a natural candidate for lithophysal application using a proper probe size and measurement time interval for receiving thermal response from a large enough, representative rock volume. A single-borehole installation is (a) simpler than a two- or multiple-borehole unit, (b) the relative positions of the temperature sensors to the heater(s) are fixed by the body of the probe, thus, they are precise and require no in situ surveying, (c) due to (a) and (b), significant cost-saving per measurement installation can be accomplished. In addition, the single-borehole method applies a relatively compact, ellipsoid-type temperature field that can be fitted into a relatively small, finite volume that is kept within the intact rock, away from a disturbed, open boundary surface.

This paper describes the measurement concept and the proof-of-principle tests of the lithophysal application of the REKA method based on numerical simulation. Support analysis for the design is carried out based on emulated temperature fields, using the Non-equilibrium, Unsaturated-saturated Flow and Transport (NUFT) software [5]. The reason for using emulated

measurements is that controlled conditions can be provided. The input properties that specify the rock model and formation in NUFT (e.g., heat conductivity, lithophysal porosity, lithophysal distribution) are known input for creating the time-dependent temperature field in the rock. A “blind” evaluation of the temperature field, representing a computer-emulated measurement, is made with the REKA V1.1 software in which the temperature field is used as an input, and the conductivity and lithophysal porosity are inverse-evaluated as output. Conclusions are drawn based on comparing the known inputs of NUFT to the blindly evaluated outputs of REKA V1.1 software. The only connection between NUFT and REKA V1.1 is provided by (a) the known geometry of the REKA probe, (b) the probe’s heating power, and (c) the emulated temperature field with space and time.

## THE REKA METHOD IN LITHOPHYSAL APPLICATION

The REKA method involves a single borehole probe with an integral heater and a temperature measurement section. The lithophysal REKA probe applies a twin-heater arrangement with a 1 m-long measurement section on a straight line between two short heater elements spaced 3m apart. The twin-heater arrangement is effectively two single-heater REKA probes comprised within one embodiment. This arrangement was found advantageous during the preliminary method analysis for lithophysal application [6] in order to integrate the uneven heat flow in the scattered rock formation. The probe arrangement is simplified for the present study, representing the short heaters with point sources and applying six temperature sensors, shown in Fig. 1. An incremental, spherical temperature field is generated by each heater of the lithophysal REKA probe. The temperature distribution along the length of the probe is recorded at the six locations hourly for 160 hrs. A trial-and-error evaluation procedure, according to the qualified REKA V1.1 software that includes the twin-heater option [7], is used to determine the unknown thermophysical properties by minimizing the root-mean-square error between the measured and the calculated incremental temperature fields with the trial thermophysical properties. Since the REKA method uses incremental temperatures generated by a small incremental heating signal, in situ measurements can be conducted under variable ambient temperatures and hydrothermal conditions.

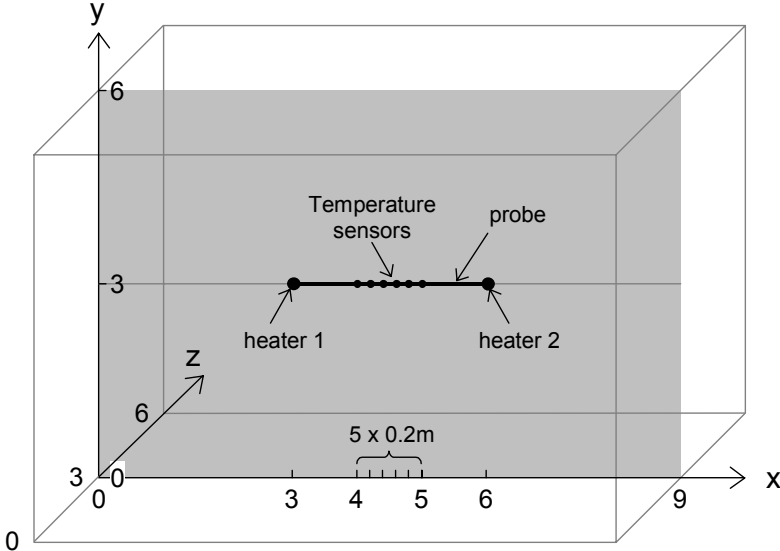


Fig. 1. Schematic REKA Probe Arrangement in a 6m×6m×9m Rock Block

### In Situ Measurement Emulation

In situ measurements are emulated using NUFT by calculating the temperature field generated by the REKA heaters shown in Fig. 1. The simulation is performed on a rock block of 9 m by 6 m by 6m, which is sub-divided into 45 X 30 X 30 elements, giving 40,500 cubes with sides of 0.20 m. This rock block size is found sufficiently large enough to contain the temperature disturbance caused by the heaters of the REKA probe without raising the temperature on the boundaries for a 160 hour time period. The rock model domain is initially filled with a double-porosity material with matrix and fracture porosities, typical for Yucca Mountain welded tuff. The matrix and fracture elements are named m-tsw35 and f-tsw35. Three cases (Case 1, 2, and 3) are analyzed by emulating three hypothetical REKA measurements using the rock without any lithophysal cavity in it. These initial cases are analyzed for checking the inverse modeling accuracy of the REKA method arrangement for this emulated measurement. The input rock hydrothermal properties and conditions are given in Tables I-IV. The goal of Cases 1-3 is to back-identify the known input rock properties from the simulated measurement fields with the REKA inverse method for baseline comparison.

Seven cases (Case 4 through 10) are analyzed with the introduction of lithophysal cavities in the rock block. The cavities are gas-filled cubic void spaces with hydrothermal properties close to that of still air, specified by the names f-dr and m-dr in Tables II, III and IV.

Cases 4 and 5 apply a regular cavity pattern shown in Fig. 2(a) for two different layer arrangements. The black squares represent cavities, while the white squares depict rock. The patterns correspond to a 0.25 lithophysal porosity, and they avoid overlap of the air cavities. A similar pattern of 0.25 lithophysal porosity but with shifted cavity positions is applied alternately in the z-direction in order to avoid overlap of the air cavities. The difference between Case 4 and 5 is in the REKA probe's position relative to the fixed cavity lattice: the two REKA heaters are

at nodes 15 and 30 in Case 4, and at nodes 16 and 31 in Case 5, representing a different relative lithophysal formation to the probe. The pattern corresponds to a 0.25 lithophysal porosity. The effective, equivalent heat conductivity of the pattern shown can be calculated in linear heat flow using elementary formulas known for layered material. Using the values for rock (m-tsw35 plus f-tsw35) conductivity of 2.0 and air (m-dr plus f-dr) conductivity of 0.026, the equivalent conductivity for the regular pattern (including both rock and air) is 1.0213 W/(m K). The goal of Cases 4 and 5 is to back-identify the effective lithophysal rock properties from the simulated measurement fields with the REKA inverse method for comparison with the expected values for lithophysal porosity (0.250) and effective conductivity (1.0213).

Cases 6 through 10 apply random cavity patterns generated according to a geometrical random cavity distribution with an average lithophysal porosity of 0.25. Fig. 2(b) is an illustration of random distribution. Although the patterns correspond to 0.25 average lithophysal porosity for the entire block, random variations are expected around the REKA probe. There is no closed solution for the effective, equivalent heat conductivity for the random patterns, but it is expected that the average of large number of evaluations is around the value of the regular pattern. The goal of Cases 6-10 is to back-identify the effective lithophysal rock properties from the simulated measurement fields for the random patterns with the REKA inverse method for comparison.

Table I. Initial properties

Cases	Initial Barometric pressure	Initial Saturation		Initial Temperature	Lithophysal pattern	Lithophysal porosity
		Matrix	Fracture			
Case1	91000	0.5	0.01	20	None	0
Case2	88720	0.962	0.01	20	None	0
Case3	88720	0.001	0.001	24	None	0
Case4	88720	0.001	0.001	24	Regular	0.25
Case5	88720	0.001	0.001	24	Regular	0.25
Case6	88720	0.001	0.001	24	RP1	0.25
Case7	88720	0.001	0.001	24	RP2	0.25
Case8	88720	0.001	0.001	24	RP3	0.25
Case9	88720	0.001	0.001	24	RP4	0.25
Case10	88720	0.001	0.001	24	RP5	0.25

**Hydrothermal properties:****Table II. Matrix Properties of the Units**

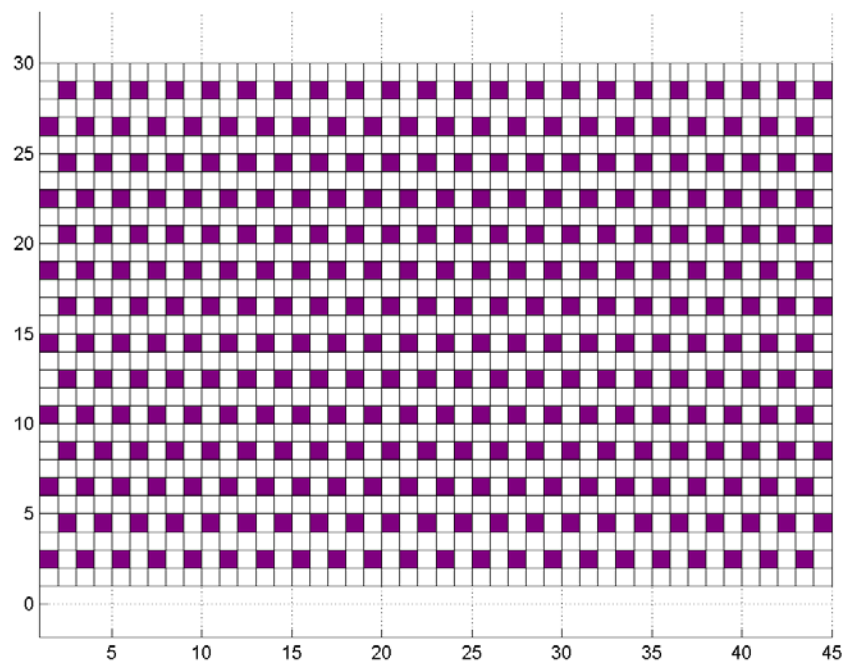
Cases	Permeability		Porosity		Van Genutchen ( $\alpha$ )	Van Genutchen ( $\beta$ )	Residual saturation	Saturated saturation
	m-tsw35	m-dr	m-tsw35	m-dr	6.44e-06	0.236	0.12	1
Case1	3.04e-17	0.5e-08	1.31e-01	0.495	6.44e-06	0.236	0.12	1
Case2	3.04e-17	0.5e-08	1.31e-01	0.495	6.44e-06	0.236	0.12	1
Case3	3.04e-17	0.5e-16	1.31e-01	0.495	6.44e-06	0.236	0.12	1
Case4	3.04e-17	0.5e-16	1.31e-01	0.495	6.44e-06	0.236	0.12	1
Case5	3.04e-17	0.5e-16	1.31e-01	0.495	6.44e-06	0.236	0.12	1
Case6	3.04e-17	0.5e-16	1.31e-01	0.495	6.44e-06	0.236	0.12	1
Case7	3.04e-17	0.5e-16	1.31e-01	0.495	6.44e-06	0.236	0.12	1
Case8	3.04e-17	0.5e-16	1.31e-01	0.495	6.44e-06	0.236	0.12	1
Case9	3.04e-17	0.5e-16	1.31e-01	0.495	6.44e-06	0.236	0.12	1
Case10	3.04e-17	0.5e-16	1.31e-01	0.495	6.44e-06	0.236	0.12	1

**Table III. Fracture Properties of the Units**

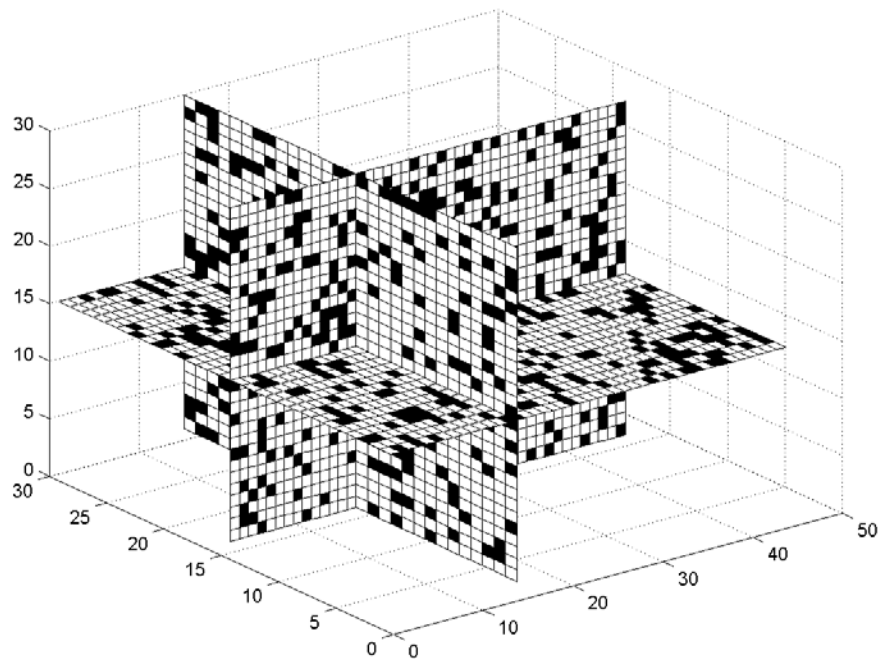
Cases	Permeability		Porosity		Van Genutchen ( $\alpha$ )	Van Genutchen ( $\beta$ )	Residual saturation	Saturated saturation
	f-tsw35	f-dr	f-tsw35	f-dr	6.44e-06	0.236	0.12	1
Case1	1.29e-12	0.5e-08	1.1e-02	0.495	6.44e-06	0.236	0.12	1
Case2	1.29e-12	0.5e-08	1.1e-02	0.495	6.44e-06	0.236	0.12	1
Case3	1.29e-16	0.5e-16	1.1e-02	0.495	6.44e-06	0.236	0.12	1
Case4	1.29e-16	0.5e-16	1.1e-02	0.495	6.44e-06	0.236	0.12	1
Case5	1.29e-16	0.5e-16	1.1e-02	0.495	6.44e-06	0.236	0.12	1
Case6	1.29e-16	0.5e-16	1.1e-02	0.495	6.44e-06	0.236	0.12	1
Case7	1.29e-16	0.5e-16	1.1e-02	0.495	6.44e-06	0.236	0.12	1
Case8	1.29e-16	0.5e-16	1.1e-02	0.495	6.44e-06	0.236	0.12	1
Case9	1.29e-16	0.5e-16	1.1e-02	0.495	6.44e-06	0.236	0.12	1
Case10	1.29e-16	0.5e-16	1.1e-02	0.495	6.44e-06	0.236	0.12	1

**Table IV. Thermal Properties of the Rock Domain**

	Solid Density Case1-10	Specific Heat Case1-10	Wet conductivity		Dry conductivity		
			Case 1-2	Case3-10	Case1 2	Case 3	Case 4 -10
f-tsw35	2.82e+01	900	2.22e-02	0.01	1.31e-02	0.01	0.01
m-tsw35	2.89e+03	900	1.996	1.99	1.18	1.99	1.99
f-dr	5.92e-01	1006	0.01	0.01	0.01	0.01	0.01
m-dr	5.92e-01	1006	0.013	0.013	0.013	0.013	0.013



(a)



(b)

Fig 2. Lithophysal Cavity Patterns: (a) Regular Pattern of a Layer(Case 4 and 5).  
(b) Random Pattern in Three Dimensions.

### Evaluation Concept of Lithophysal Porosity, $\varphi_l$

The lithophysal porosity can be obtained from a single in situ REKA measurement if the baseline, non-lithophysal rock properties are known. Based on the measured temperature field  $TM(x,t)$  acquired by the REKA probe, and using the REKA V1.1 software with the built-in conduction-only forward prediction model, the effective thermophysical properties can be determined:

$$TM(x,t) \rightarrow \begin{cases} k_{eff} \\ \alpha_{eff} \end{cases} \quad (\text{Eq. 1})$$

Since  $k_{eff}$  is evaluated from a measured temperature field,  $TM(x,t)$ , the effect of heat radiation across cavities, a significant transport component when the cavity size is large, is included in the in situ value. Note that the simulated temperature fields in this paper do not include these effects.

The ratio of conductivity to diffusivity is  $(\rho c_p)_{eff}$ . Using the definition of the lithophysal volumetric porosity, and assuming that the lithophysae are filled with gas, the following equation can be written :

$$(\rho c_p)_{eff} = \frac{k_{eff}}{\alpha_{eff}} = (\rho c_p)_{rock} (1 - \varphi_l) + (\rho c_p)_{gas} \varphi_l, \quad (\text{Eq. 2})$$

Since the density of gas is negligible when compared to that of rock, Eq. (2) can be simplified by eliminating the last term in the right-hand side. Through this simplification, the lithophysal porosity is:

$$\varphi_l = 1 - \frac{(\rho c_p)_{eff}}{(\rho c_p)_{rock}} = 1 - \frac{k_{eff}}{\alpha_{eff} (\rho c_p)_{rock}} \quad (\text{Eq. 3})$$

In order to evaluate  $\varphi_l$ , rock density and heat capacity need to be given for  $(\rho c_p)_{rock}$  into Eq. (3). This term may be available from laboratory measurement results. Note that  $\varphi_l$  is affected by both conductivity and specific heat, showing the complexity of the thermal behavior of porous media.

### Numerical Method Verification

The method of analysis used in this study is verified based on Cases 1 through 3. (For these study cases, both the calculations and the lithophysal porosity are 2D values.) The results of the emulated measurement temperature field obtained using NUFT as inputs and the inverse-modeled temperature field for Case 3 is shown in Fig. 3(a) and 3(b). The thick lines are temperature curves from NUFT using the input values of thermal conductivity and diffusivity, while the thin lines are the temperature curves calculated using the thermal conductivity and diffusivity obtained from the best fit to the NUFT temperature field, as determined, while the thin lines are the curves calculated, as best fit, by the REKA V1.1 inverse modeling software.

The graphs are standard outputs of the software. The effective thermal conductivity and diffusivity values are depicted in Fig. 3, and summarized for all cases in Table V.

Table V. Results after post processing the results obtained from Reka v 1.1

Cases	Conductivity (W/m.k)	Diffusivity (m^2/s)	T <sub>AV</sub> (degree C)	RMS error (degree C)
Case1	1.5477	6.2450e-07	20.00	2.4184e-003
Case2	1.9779	7.1750e-07	20.00	1.6094e-003
Case3	2.0010	8.9347e-07	24.000	8.1434e-004
Case4	1.0367	6.2200e-07	24.0070	4.3171e-002
Case5	1.0367	6.2200e-07	24.0070	4.3167e-003
Case6	0.8412	5.5039e-07	24.0070	2.1462e-002
Case7	1.0677	7.3294e-07	24.0065	6.0646e-003
Case8	0.7128	4.7044e-07	24.0100	2.5494e-002
Case9	1.0259	5.8745e-07	24.0042	5.5671e-003
Case10	0.9489	6.3343e-07	24.0060	1.2274e-003

The expected conductivity for Case 1 is 1.59, corresponding to a saturation of the rock at around 50%. This value is similar to the 1.55 result from the REKA V1.1 evaluation. The expected conductivity for Case 2 is 1.97 for a saturation of 96%. This value is also in agreement with the REKA V1.1 result of 1.98. The expected conductivity for the low-saturation Case 3 is 1.99 since both the dry and wet conductivities were set to that value in the NUFT input deck. The result from the REKA V1.1 software is almost identical, 2.00. These results show that the probe arrangement is correctly modeled and the domain as well as time discretization are acceptable. Case 3 is used as a baseline case and for supplying the  $(\rho c_p)_{rock}$  value for the lithophysal evaluations. It was selected to avoid uncertainties associated with the movement of water in the system being modeled.

### Measurement Arrangement Verification

The lithophysal REKA measurement arrangement is verified based on Cases 4 and 5. The result of the emulated measurement temperature field obtained using NUFT as inputs and the inverse-modeled temperature field for Case 4 is shown in Fig. 4(a) and 4(b) as an example. The expected conductivity for Cases 4 and 5 is 1.0213 as discussed in the foregoing. This is in excellent agreement, within 1.5%, with the results of 1.0367 from the REKA V1.1 software for Cases 4 and 5. This agreement verifies that the measurement arrangement although based on two superimposed spherical temperature fields, closely represent a linear heat flow case. This verification justifies the design arrangement with the relatively widely spaced heaters and the 1m minimum distance between the center of the heaters and the closest temperature sensor station.

The expected lithophysal porosity for Cases 4 and 5 is 0.25 as discussed in the foregoing. For comparison, it is necessary to process the results in Table V using Eq. (3). The  $(\rho c_p)_{rock}$  value for the rock without the lithophysae is conveniently taken from the baseline Case 3 as the ratio of conductivity to diffusivity, giving  $(\rho c_p)_{rock} = 2.24 * 10^6$ . Using this value in Eq. (3), the lithophysal porosities are evaluated and given in Table VI.

Table VI. Lithophysal Porosities using Eq. (3)

Cases	$\rho_C$	$\varphi_L$
Case3	2.24e+06	0
Case4	1.67e+06	0.256
Case5	1.67e+06	0.256
Case6	1.53e+06	0.318
Case7	1.46e+06	0.349
Case8	1.515e+06	0.324
Case9	1.75e+06	0.220
Case10	1.50e+06	0.331

The post-processed lithophysal porosity from the REKA method is in excellent agreement, within 2.5%, with the expected value. This agreement further verifies the methodology and justifies the measurement arrangement.

### Study of the Effect of Random Lithophysal Patterns

Little is known about the nature of non-steady-state heat and moisture flow in lithophysal rock formation. Encouraged by the efficiency of the NUFT and REKA V1.1 combination to study a variety of arrangements, a Monte-Carlo analysis has commenced as a university research project to gain a better understanding. Cases 6 through 10 are sample results of this effort. A different, random cavity pattern is generated for each case with an average lithophysal porosity of 0.25 for the whole rock domain. The result of the emulated measurement temperature field obtained using NUFT as inputs and the inverse-modeled temperature field for Case 10 is shown in Fig. 5(a) & 5(b) as an example. The conductivity results, given in Table V, show a slight variation around an average of 0.953. This value is within 6.5% of the expected value for the same lithophysal porosity, but with a regular cavity pattern. The lithophysal porosity evaluation values, given in Table VI, vary around an average of 0.308. This value is within 23% of the expected value for the entire volume in the domain. The results for the five random samples are encouraging. Although too few in number for drawing conclusions about the statistics, they serve as demonstrations of the uncertainties of the single measurements when the active measurement area is surrounded with a random pattern of the lithophysae.

### CONCLUSIONS

A method is presented, based on the NUFT and REKA V1.1 combination, to study the nature of non-steady-state heat flow during a single-borehole REKA thermal probe thermophysical measurement in solid as well as lithophysal rock formation with a regular and a random lithophysal pattern. The results prove the principle of the REKA method application in lithophysal formation.

The numerical evaluation results, based on the use of two qualified software packages, show that the presented REKA probe arrangement designed for lithophysal thermophysical properties identification is correctly modeled and the domain as well as time discretizations are acceptable.

The REKA probe arrangement can be used to inverse-identify the effective heat conductivity and thermal diffusivity, and through these values, the lithophysal porosity of a regular lithophysal cavity pattern can be determined. This numerical verification justifies the design arrangement with the relatively widely spaced heaters and the 1m minimum distance between the center of the heaters and the closest temperature sensor station.

A method is presented, based on the NUFT and REKA V1.1 combination, to study the nature of non-steady-state heat in lithophysal rock formation with a random lithophysal pattern. A Monte-Carlo analysis is needed to increase the number of random samples for statistical evaluation. The five sample results presented are encouraging.

## REFERENCES

1. Yucca Mountain Science and Engineering Report, DOE/RW-0539, 2001.
2. Danko, G., Creech,H., Phillips, J., and Tippabhatla, S.,(1998). "In Situ Reka Probe Measurements at Fran Ridge and in the ESF at Yucca Mountain," Proceedings, 8th Int. High-Level Radioactive Waste Management Conference, Las Vegas, NV, pp. 54-56.
3. Fran Ridge Report – LLNL with REKA application, Large Block Test Final Report TDR-NBS-HS-000012, UCRL-ID-132246, July 2001.
4. Danko, G., Bahrami, D., and Adu-Acheampong, A., (2001). "In Situ Thermophysical Properties Measurements under Hydrothermal Disturbances at DST," Proceedings, 9th Int. High-Level Radioactive Waste Management Conference, Las Vegas, NV, pp. 1-4.
5. NUFT Flow and Transport code V3.0s, Software Configuration Management, Yucca Mountain Project – STN: 10088-3.0S-00 Prepared by Lawrence Livermore National Laboratory, September 2000.
6. SN Task 13 Scientific Notebook UCSSN-UNR-013, Vol. 2, pp 60-68.
7. REKA V1.1 Qualified Software," Rapid Evaluation of K and alpha", Software Configuration Management, Yucca Mountain Project -- STN: 10383-1.1-00, January 2001.

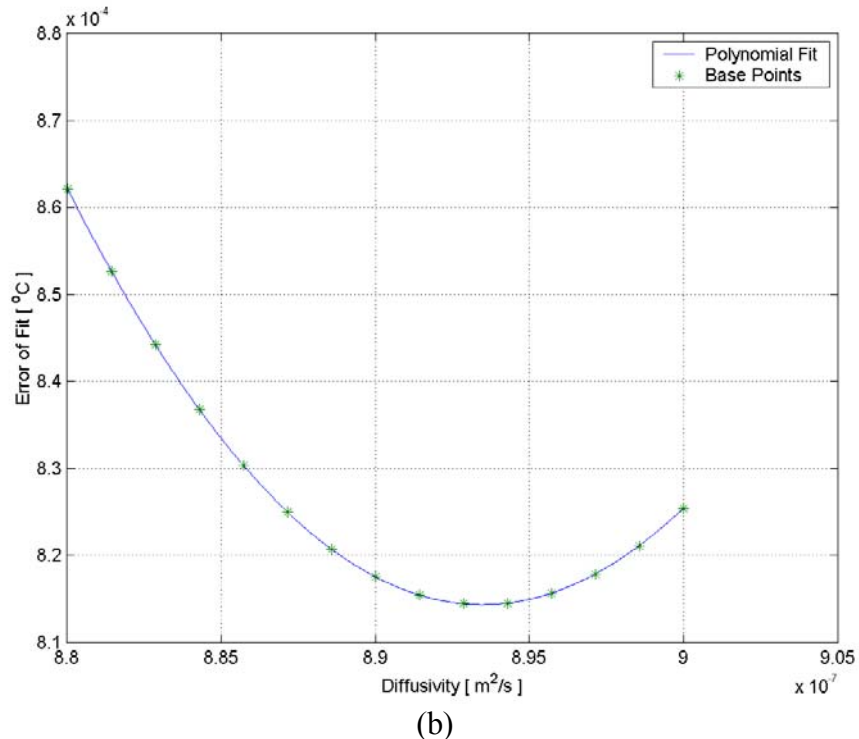
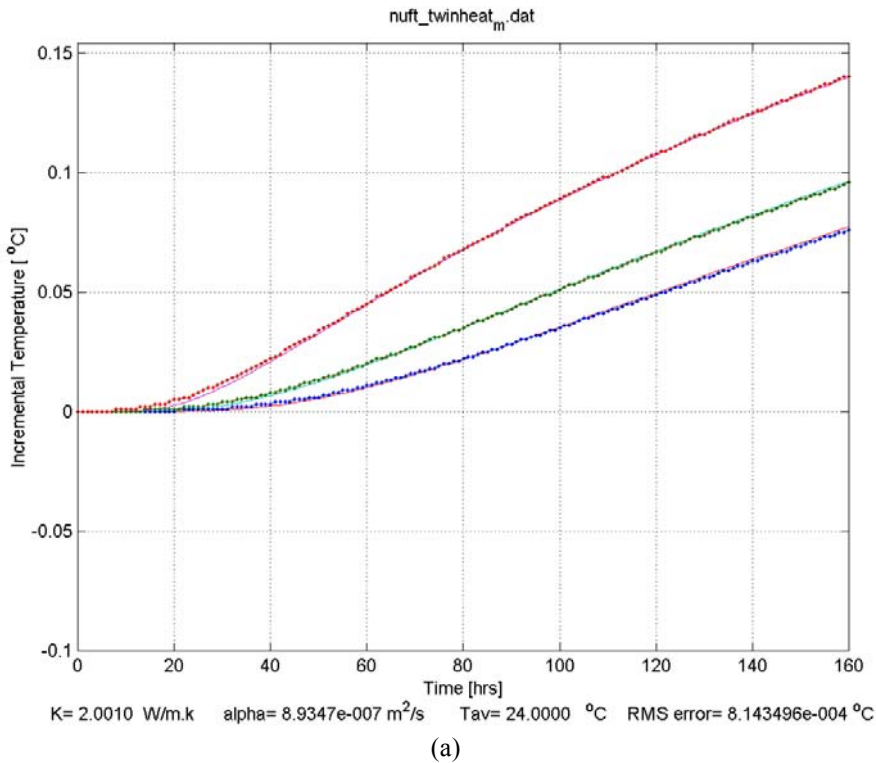


Fig. 3. Inverse Evaluation Results of Case 3 (Solid rock, baseline case). (a) Thick dotted lines are the inputs to REKA V1.1 from NUFT. Thin lines are best-fitted curves generated by REKA 1.1. (b) Error of fit curve generated during inverse optimization by REKA V1.1.

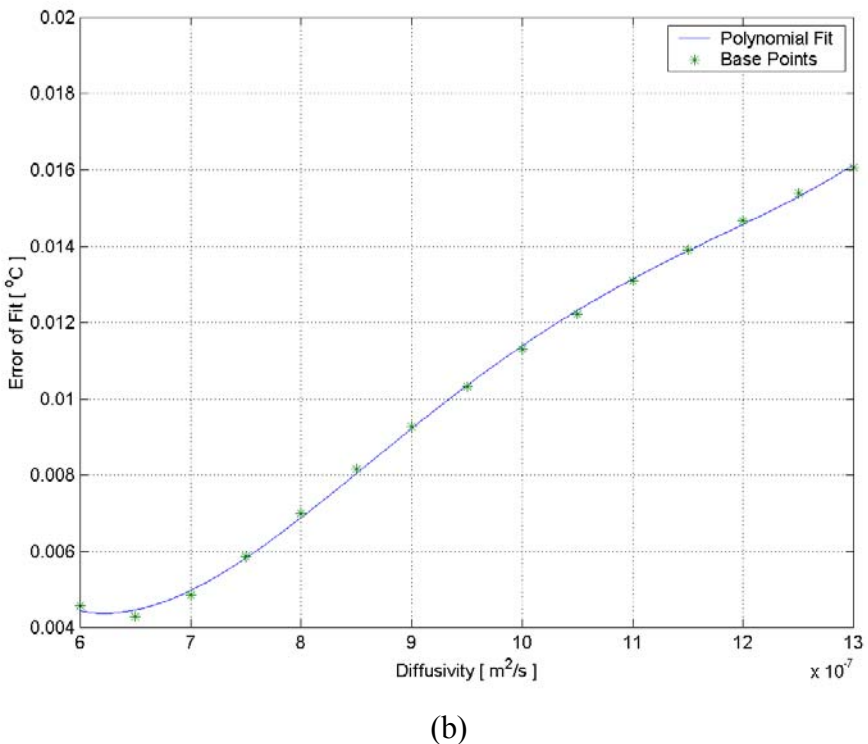
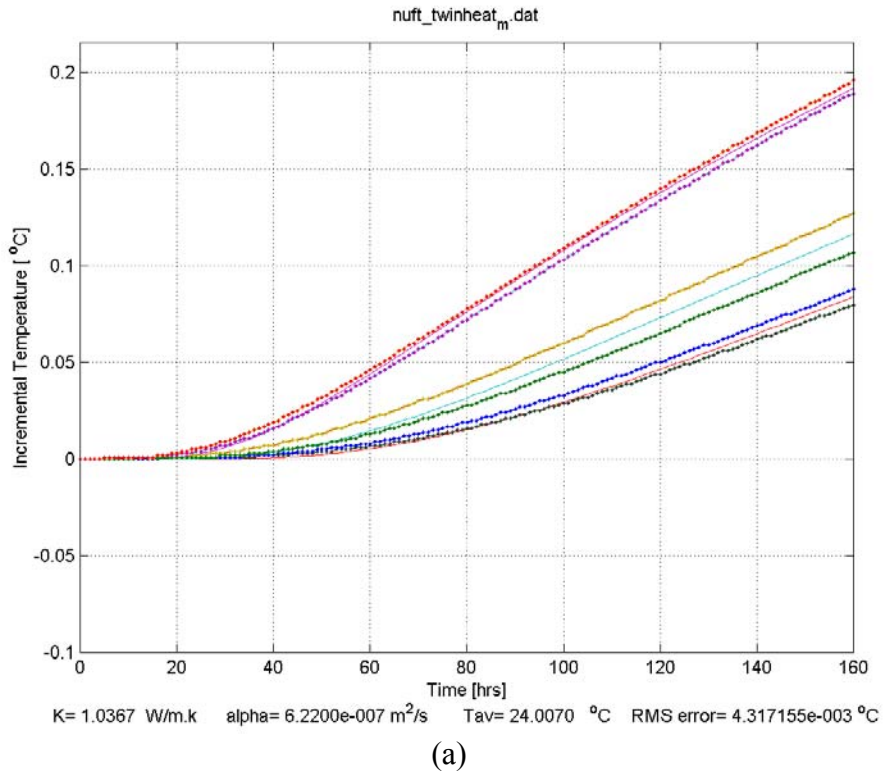
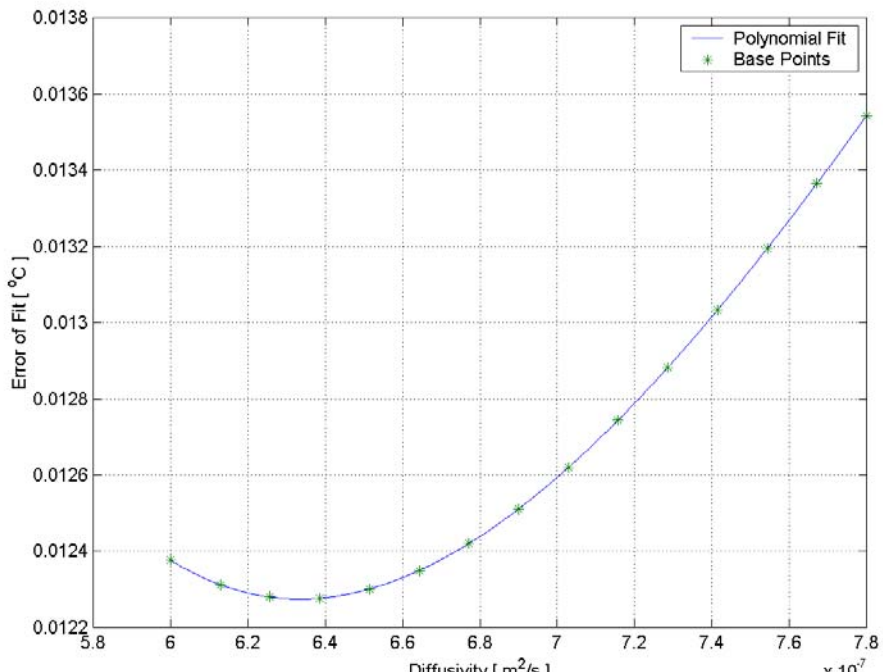
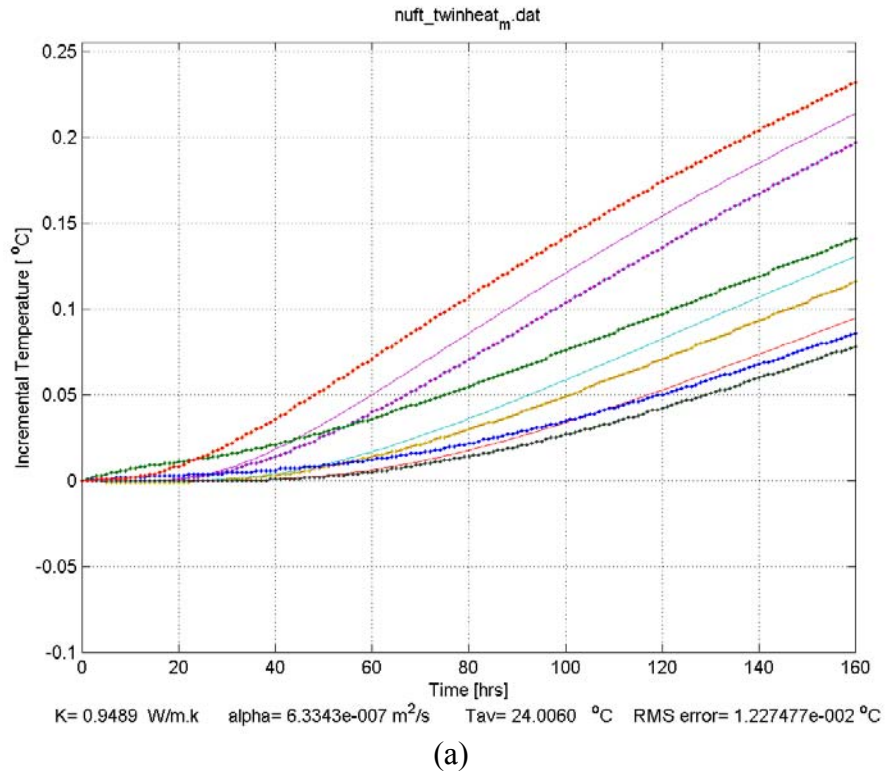


Fig. 4. Inverse evaluation results of Case 4 (Regular Lithophysal Pattern)

(a) Thick dotted lines are the inputs to REKA V1.1 from NUFT. Thin lines are best-fitted curves generated by REKA V1.1.

(b) Error of fit curve generated during inverse optimization by REKA V1.1.



(b)

Fig. 5. Inverse evaluation results of Case 10 (A typical random lithophysal pattern).

(a) Thick dotted lines are the inputs to REKA V1.1 from NUFT. Thin lines are best-fitted curves generated by REKA V1.1.

(b) Error of fit curve generated during inverse optimization by REKA V1.1.